Molecular Crystals and Liquid Crystals

Publication details, including instructions for authors and subscription information:
http://www.tandfonline.com/loi/gmcl20

Dynamics of Light Induced Reorientation of Nematic Liquid Crystals in Spatially Confined Beams

Etienne Brasselet [a], Tigran Galstian [b] & Louis Dubé [c]

[a] Laboratoire de Photonique Quantique et Moléculaire (UMR 8537), Cachan Cedex, France

[b] Département de Physique, de Génie Physique et d'Optique, Université Laval, Cité Universitaire, Québec, Canada

[c] Laboratoire de Dynamique des Ions, des Atomes, et des Molécules, Université Pierre et Marie Curie, Paris Cedex 05, France

Version of record first published: 18 Oct 2010

To cite this article: Etienne Brasselet, Tigran Galstian & Louis Dubé (2004): Dynamics of Light Induced Reorientation of Nematic Liquid Crystals in Spatially Confined Beams, Molecular Crystals and Liquid Crystals, 421:1, 69-80

To link to this article: http://dx.doi.org/10.1080/15421400490501400

Mol. Cryst. Liq. Cryst., Vol. 421, pp. 69–80, 2004

ISSN: 1542-1406 print/1563-5287 online
DOI: 10.1080/15421400490501400

Taylor & Francis
Taylor & Francis Group

DYNAMICS OF LIGHT INDUCED REORIENTATION OF NEMATIC LIQUID CRYSTALS IN SPATIALLY CONFINED BEAMS

Etienne Brasselet
Laboratoire de Photonique Quantique et Moléculaire (UMR 8537), ENS de Cachan, 94235 Cachan Cedex, France

Tigran Galstian
Département de Physique, de Génie Physique et d'Optique, Université Laval, Cité Universitaire, Québec, Canada G1K7P4

Louis J. Dubé
Laboratoire de Dynamique des Ions, des Atomes, et des Molécules, Université Pierre et Marie Curie, 4 Place Jussieu, 75252 Paris Cedex 05, France

Optically induced reorientation dynamics in a nematic liquid crystal is investigated for circularly polarized laser beams with spot sizes smaller than the sample thickness. Various dynamical regimes, such as periodic, quasi-periodic, intermittent, self-organized and possibly chaotic regimes are observed. The role finite beam size is identified and a qualitative interpretation based on the spatial walk-off of the ordinary and extraordinary beams arising from double refraction phenomenon is proposed.

Keywords: finite-beam excitation; instabilities; light angular momentum; molecular reorientation; walk-off effects

INTRODUCTION

Liquid crystals offer a versatile system for the experimental and theoretical study of a variety of non-linear phenomena. In particular, the nonlinear optics of liquid crystals as become a well-established research field [1–4]

Address correspondence to Etienne Brasselet, Laboratoire de Photonique Quantique et Moléculaire (UMR 8537), ENS de Cachan, 94235 Cachan Cedex, France. E-mail: ebrassel@lpqm.ens-cachan.fr

including light-induced phase transitions [5,6] and stimulated light scattering [7]. In the past decade, considerable efforts have been made to achieve a deeper understanding of nonlinear mechanisms of the light-liquid crystal interaction. The case of an homeotropic cell of nematic liquid crystal (NLC) under a light field excitation has received special attention and the ensuing studies have led to quantitative theoretical descriptions capable of retrieving the main features of the various dynamical regimes observed until then. A key example is the case of the normally incident elliptically polarized light leading to a rich variety of molecular orientational dynamics [8,9], with the particular case of circularly polarized excitation, which exhibits a nontrivial sequence of successive bifurcations [10,11]. The transition to chaos via a cascade of gluing bifurcations by an ordinary wave at oblique incidence [12–15] is yet another example. More recently, it was shown that a strongly astigmatic laser beam can induce non linear oscillations due to the competition of spin and orbital angular momentum of light [16]. In particular, chaotic rotation associated with intermittency was identified

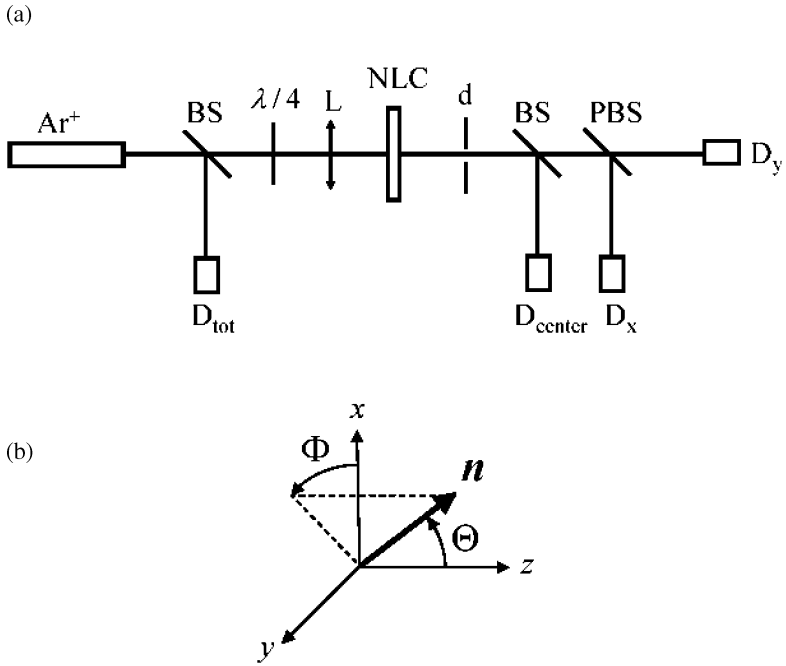

FIGURE 1 (a) Experimental set-up. Ar^+: Argon ion laser; BS: beam splitter; $\lambda/4$: quarter wave plate; L: lens; NLC: nematic liquid crystal film; d: diaphragm; PBS: polarizing beam splitter; D_i: photodetectors. (b) Definition of the director n by the spherical angles Θ and Φ.

in such a system [17]. However, due to the complexity of the problem, most of the corresponding theoretical models have assumed an infinite plane wave (IPW) excitation, an assumption not justified in many experiments where the beam size is comparable or less than the NLC film thickness. Despite several attempts to describe the finite beam size effects, only the linearly polarized excitation, where the long-term behavior is time-independent, has been studied in some detail [5,18–20] and it is fair to say that a complete dynamical model is still lacking.

In this work, we report observations of the influence of transverse effects on the molecular reorientation dynamics induced by circularly polarized and spatially confined beams. First, we present the experimental set-up used to probe finite beam size effects on the light-induced reorientation dynamics. The role of *self-induced walk-off* is pointed out and a qualitative criterion is proposed to estimate the importance of finite beam size effects to the observed dynamics under a given set of experimental conditions (beam diameter, cell thickness and reorientation amplitude).

We will refer to the molecular dynamics by means of the vector field that represents the average local orientation of the molecules defined by the unit vector n, called the director. Its orientation is given by the two usual spherical angles Θ and Φ, namely $\mathrm{n} = (\sin\Theta\cos\Phi,\ \sin\Theta\sin\Phi,\ \cos\Theta)$ as depicted in Figure 1b.

CONFRONTATION EXPERIMENT-THEORY

The sample under study is a film of nematic liquid crystal E7 (from Aldrich) enclosed between two glass substrates and the film thickness is $L = 100\,\mu\mathrm{m}$. The substrates are coated with CTAB surfactant for homeotropic alignment, i.e. an alignment perpendicular to the surfaces of the substrates. The excitation laser beam, obtained from an Ar^+ laser operating at 514.5 nm in the TEM_{00} mode, is focused at normal incidence on the sample by the lens L (see Fig. 1a). At the sample location the intensity profile has a Gaussian shape, d being the beam diameter at e^{-2}. The polarization state of the excitation light is made circular using a quarter wave plate ($\lambda/4$) placed before the lens L (see Fig. 1a). The director reorientation dynamics is retrieved by the analysis of the central part of the beam emerging from the sample after the diaphragm d. Photodiodes D_{center}, D_{x}, D_{y} collect, respectively, the total intensity of the central part of the beam, I_{center}, and the corresponding vertical and horizontal components of the electric field, I_{x} and I_{y} ($I_{\mathrm{center}} = I_{\mathrm{x}} + I_{\mathrm{y}}$). The excitation intensity I_{tot} is monitored with the photodiode D_{tot}. Data acquisition frequency is 5 Hz and the increment of normalized excitation intensity is $\delta\tilde{I} = 0.05$, where $\tilde{I} = I_{\mathrm{tot}}/I_F$, and I_F denotes the Fréedericksz transition threshold for circularly polarized light.

The time series $I_{\text{center}}(t)$ contain explicit information on $\mathbf{\Theta}$ only. This is because the level of self-focusing arising from the finite beam size is governed by the amount of reorientation ($\mathbf{\Theta}$) and that only the central part of the total output intensity is collected by D_{center}. On the other hand, the time series I_{x} and I_{y} contain explicit information on both $\mathbf{\Theta}$ and $\mathbf{\Phi}$ since the intensity of the x and y electric field components depend on both the shape ($\mathbf{\Theta}$) and the orientation ($\mathbf{\Phi}$) of the output polarization ellipse and on $I_{\text{center}}(t)$. The normalized intensities with respect to $I_{\text{center}}(t)$, $i_{\text{x}} \equiv I_{\text{x}}/\ I_{\text{center}}$ and $i_{\text{y}} \equiv I_{\text{y}}/I_{\text{center}}$, contain for their part only explicit information on the polarization ellipse. Since $i_{\text{x}} \equiv 1 - i_{\text{y}}$, these time series possess the same dynamical information, we shall refer to any of these quantities as $i(t)$.

Figure 2 shows the phase space reconstructed from the observed time series (on the left), namely $i(t + \tau_d)$ versus $i(t)$, where τ_d is a time delay chosen conventionally as the first zero of the auto-correlation function, for $\tilde{I} \leq 1.25$ for a geometrical aspect ratio $\delta \equiv d/L = 0.24$. On the right part of this figure, the Fourier power spectra $I_{\text{center}}(\omega)$ and $i(\omega)$ are calculated from the time series $I_{\text{center}}(t)$ and $i(t)$. In the left column of Figure 2, a fine closed-loop in phase space is the sign of a uniform precession regime without nutation, i.e. the polarization ellipse is continuously rotating while keeping its shape constant. On the other hand, a time dependent shape of the polarization ellipse is identified by a thickening of the closed-loop. The frequency labeling appearing in the Fourier spectra, on the right part of Figure 2, takes into account our previous remarks. Namely, $I_{\text{center}}(t)$ contains information on the self-focusing of the beam, that is, on the total light-induced phase shift $\mathbf{\Delta}$ between the *o*- and *e*-waves, and the corresponding frequency is labeled f_1. Furthermore, we have mentioned earlier that $i(t)$ contains only explicit information on the shape ($\mathbf{\Theta}$) of the polarization ellipse and its orientation ($\mathbf{\Phi}$) but not on the self-focusing, in distinction to the experimental values of $I_{\text{x}}(t)$ and $I_{\text{y}}(t)$. Thus, since the shape of the rotating polarization ellipse is almost constant in the regular precession regime with frequency f_0 the corresponding frequency of $i(\omega)$ is accordingly labeled $2f_0$ since the polarization ellipse is invariant by a rotation of π. A summary of the observed bifurcation scenario is given below.

For $\tilde{I} \leq 1$ we have no reorientation as expected. At $\tilde{I} = 1$, the system experiences a subcritical Hopf bifurcation that corresponds to the Fréedericksz transition and, after a transient, it settles to a stationary uniform precession regime. In this case, the phase space is almost a perfect circle (Fig. 2a) and the Fourier spectra $i(\omega)$ exhibits a single frequency $2f_0$. Significant nutation appears for $\tilde{I} > 1$ as the system explores a progressively larger volume of phase space (Figs. 2b–c). A look at the reconstructed phase space for $\tilde{I} = 1.15$ (Fig. 2c) indicates that a dynamical transition has just taken place. This corresponds to the secondary

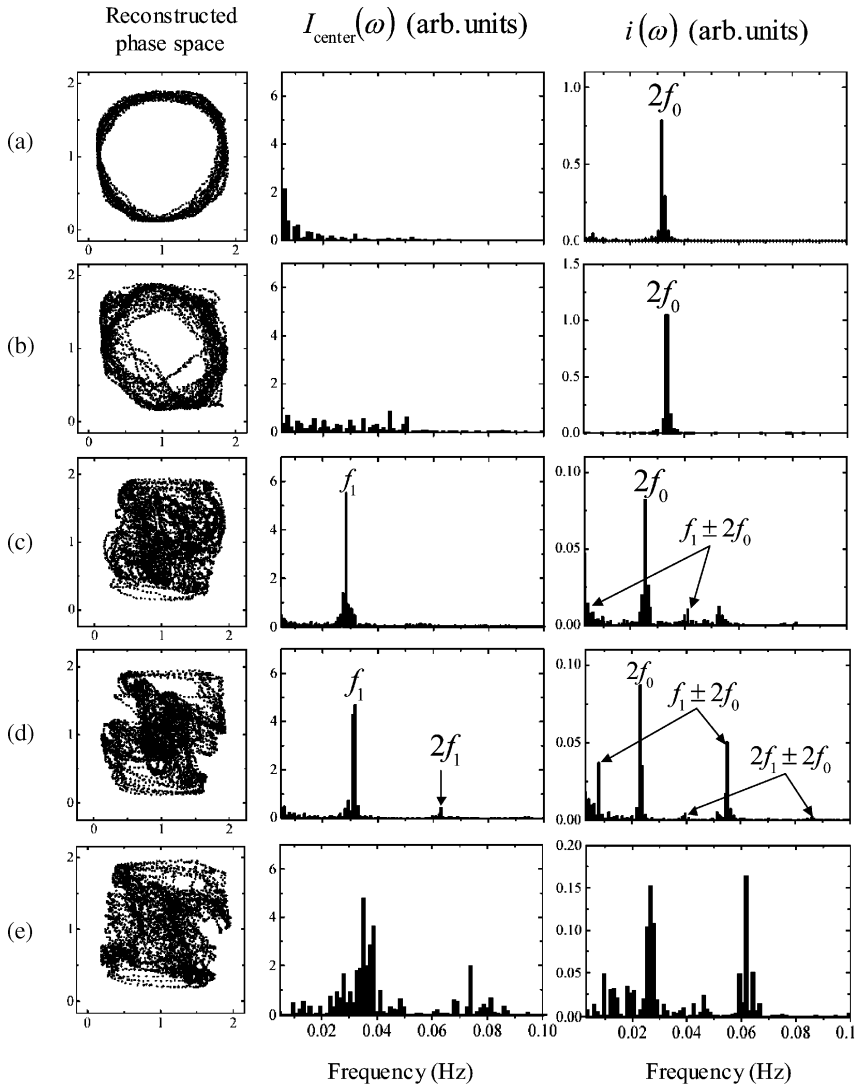

FIGURE 2 Experimental scenario in the case $L = 100\,\mu\text{m}$ with $\delta = 0.24$. From left to right: the reconstructed phase space $i(t + \tau_d)$ versus $i(t)$ and the Fourier power spectra of $I_{\text{center}}(t)$ and of $i(t)$. The time delay is taken as $\tau_d = 8\text{s}$. (a) $\tilde{I} = 1$; (b) $\tilde{I} = 1.10$; (c) $\tilde{I} = 1.15$; (d) $\tilde{I} = 1.20$; (e) $\tilde{I} = 1.25$.

instability observed in [10], which was attributed to the longitudinal asymmetry of optical angular momentum transfer to the NLC [10,11]. The dynamical regime born through this instability is clearly identified from

the Fourier spectra (Fig. 2c) just above the corresponding threshold. The NLC molecules are now rotating around the z-axis ($2f_0$) with a large periodic nutation (f_1). This continuous transition from a periodic regime towards quasi-periodicity emphasizes the second-order nature of the transition, which has the character of a supercritical Hopf bifurcation [11]. On the other hand, the occurrence of the harmonics $f_1 \pm 2f_0$ in the spectra $i(\omega)$ is a direct manifestation of the nonlinear coupling between the two degrees of freedom Θ and Φ. A further increase of $\tilde{I}$ strengthens the nonlinear coupling between Θ and Φ as demonstrated by Figure 2d where the harmonics $f_1 \pm 2f_0$ now make an important contribution to the spectra $i(\omega)$. In addition, the nonlinear character of the nutation dynamics is observed in the spectrum $I_{\text{center}}(\omega)$ through the appearance of the second harmonic $2f_1$. This allows the identification of two additional frequencies in the spectrum $i(\omega)$, namely the harmonics $2f_1 \pm 2f_0$, which appear through the nonlinear coupling between polar and azimutal degrees of freedom. In fact, this sequence of dynamical regimes is correctly predicted from the IPW model (see Fig. 3a–d), which is reported in details in Ref. [21]. However, for higher intensities, we observe a transition from a quasi-periodic to an irregular regime (Fig. 2d–e), this regime being characterized by a spectral broadening around discrete frequencies for sufficiently high excitation intensities (Fig. 2e). Such a transition was not observed experimentally for higher values of δ ($\delta > 0.4$), thus our knowledge of the bifurcation scenario in the IPW limit suggest that this dynamical behavior arises from the finiteness of the beam (for $\delta < 0.4$).

In the strong excitation regime, when the intensity is increased beyond the appearance of the irregular regime, the system exhibits a novel dynamical behavior. This is illustrated in Figure 4 where the reconstructed phase space $i(t + \tau_d)$ versus $i(t)$ and the time series $i(t)$ are shown for $\delta = 0.25$ in the range $1.45 \leq \tilde{I} \leq 1.55$. At $\tilde{I} = 1.45$, the irregular regime labeled "regime 1" in (Figure 4a–b) is observed. At still higher intensity, $\tilde{I} = 1.50$, this regime coexists with another distinct regime labeled "regime 2" in (Figure 4b–c). The system alternates between these two regimes for durations that appear almost random. We believe that this is the first time that such an intermittent behavior is reported in this excitation geometry. At $\tilde{I} = 1.55$, the dynamics of the system is now definitely restricted to "regime 2". This transition is associated with self-organization: it appears that the dynamics could be described with two principal frequencies (a low and a high frequency) that are clearly visible in Figure 4c. The high frequency component of $i(t)$ is associated with an almost periodic large amplitude variations of the signal $I_{\text{center}}(t)$ (not shown here, see [21] for more details). We observed that these rapid oscillations correspond to cycles of expansion and contraction of several rings of self-diffraction, that is a nutation with large amplitude. On the other hand, the low

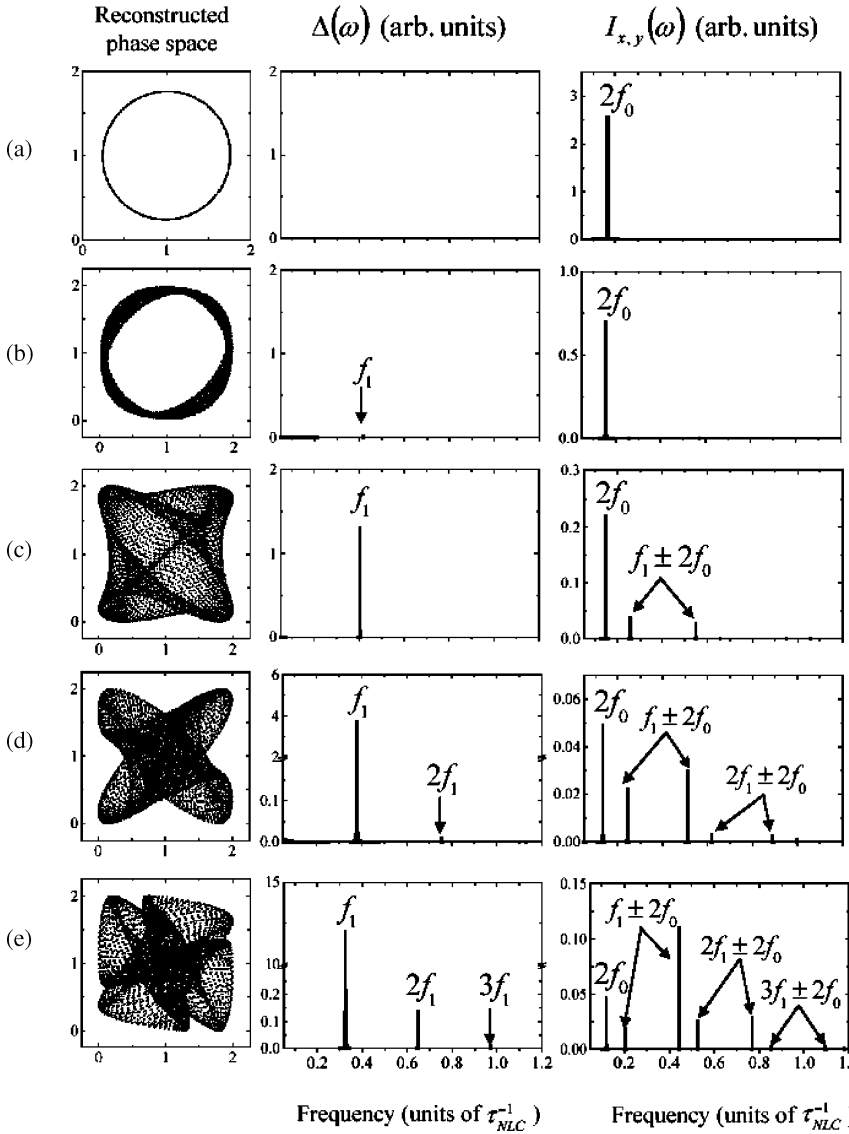

FIGURE 3 Calculated scenario in the case $L = 100\,\mu\text{m}$ with the IPW model. From left to right: the reconstructed phase space $I_{x,y}(t + \tau_d)$ versus $I_{x,y}(t)$ and the Fourier power spectra of $\Delta(t)$ and of $I_{x,y}(t)$ where $I_{x,y}(t) = \left|E_{x,y}\right|^2(z = L, t)$. The time delay is taken as $\tau_d = 1.5\tau_{NLC}$ where τ_{NLC} is a characteristic reorientation time for the NLC cell. (a) $\tilde{I} = 1.20$; (b) $\tilde{I} = 1.45$; (c) $\tilde{I} = 1.50$; (d) $\tilde{I} = 1.60$; (e) $\tilde{I} = 1.70$.

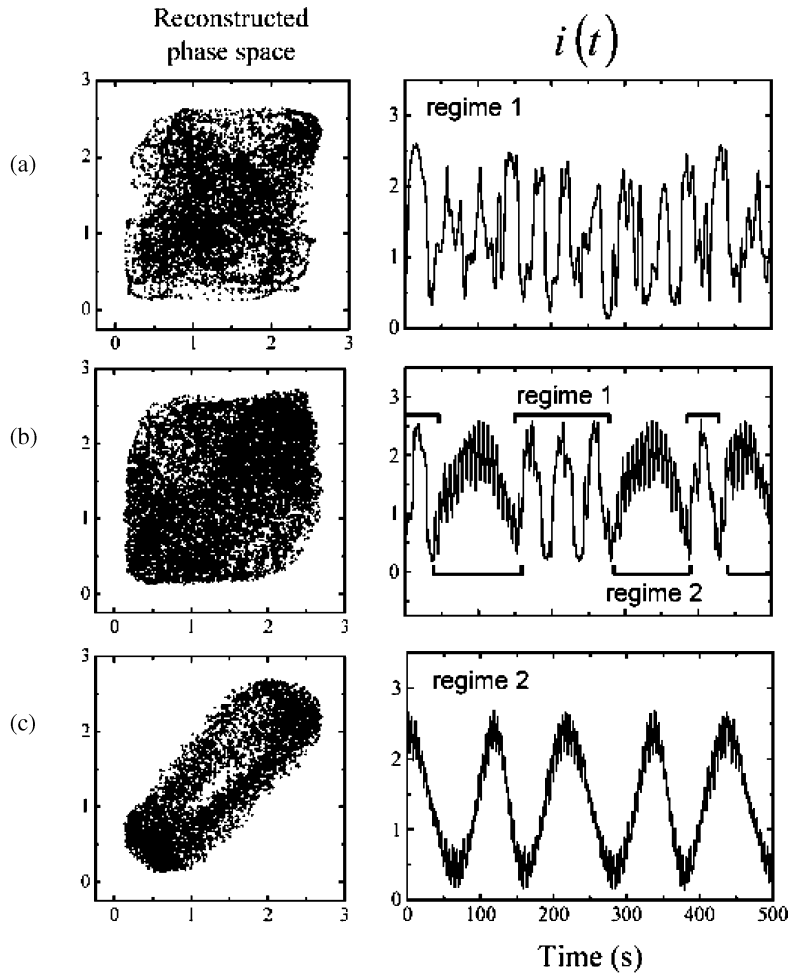

FIGURE 4 Experimental reconstructed phase space $i(t+\tau_d)$ versus $i(t)$ for a cell thickness $L = 100\,\mu\text{m}$ with $\delta = 0.25$ with $\tau_d = 8\text{s}$ (left) and the corresponding time series $i(t)$ (right). (a) $\tilde{I} = 1.45$; (b) $\tilde{I} = 1.50$; (c) $\tilde{I} = 1.55$.

frequency component corresponds to a precession regime whose frequency is several times slower than the precession rate of the uniform regime just above the Fréedericksz transition. This slowing down of the rotational motion is due to the fact that the effective rotational viscosity coefficient scales as $\sin^2 \Theta$. Finally, in all cases, a first-order transition to a largely reoriented regime occurs when the intensity is sufficiently high as reported in previous work [5,8,11,22].

These results show that for a sufficiently small beam diameter (in comparison to the film thickness), the bifurcation diagram is qualitatively modified with respect to the IPW predictions [21]. The underlying physical mechanism of this phenomenon should thus be clarified. Although it is known that director reorientation profiles may essentially be three dimensional (3D) when light beam is narrower that the film thickness [1], this is not sufficient to explain, at least qualitatively, the occurrence of new dynamical regimes since the 3D character of the reorientation has been demonstrated even in the IPW limit (both theoretically [8,23] and experimentally [24]) without such dynamics. In what follows, a qualitative physical interpretation, based on the self-induced walk-off phenomenon, is proposed.

DISCUSSION

The physics of the problem has led us to look for an interpretation based on the walk-off phenomenon that occurs in the optically anisotropic and which has been found to produce instabilities in other dynamical context, e.g. laser dynamics and optical resonators ([25] and references therein). The incident flow of energy is split into an ordinary flow propagating along the z-axis and an extraordinary one traveling at oblique incidence when the uniaxial NLC is reoriented. Since the reorientation is induced by the light itself, we should refer to this process as *self-induced walk-off*. This situation is schematically pictured in Figure 5. The non-uniform walk-off $\rho(z)$ is expressed as a function of the angle $\beta(z)$ between the e-Poynting vector and the z-axis (Fig. 5a) as

$$\rho(z) = \int_0^z \tan[\beta(z')]dz'. \tag{1}$$

The area $A(z)$ over which the o- and e-beams of diameter d overlap (shaded area in Fig. 5b) can be written as a function of $\rho(z)$ by

$$A(z) = d^2[\pi - 2\alpha(z) - \sin 2\alpha(z)]/4 \tag{2}$$

with

$$\alpha(z) = \arcsin[\rho(z)/(\delta L)]. \tag{3}$$

The relative amount of mismatch of the overlap area, $[A(0) - A(L)]/A(0)$, may define a measure of the walk-off effects. A zeroth-order approximation of this quantity can be obtained from the knowledge inferred from the IPW

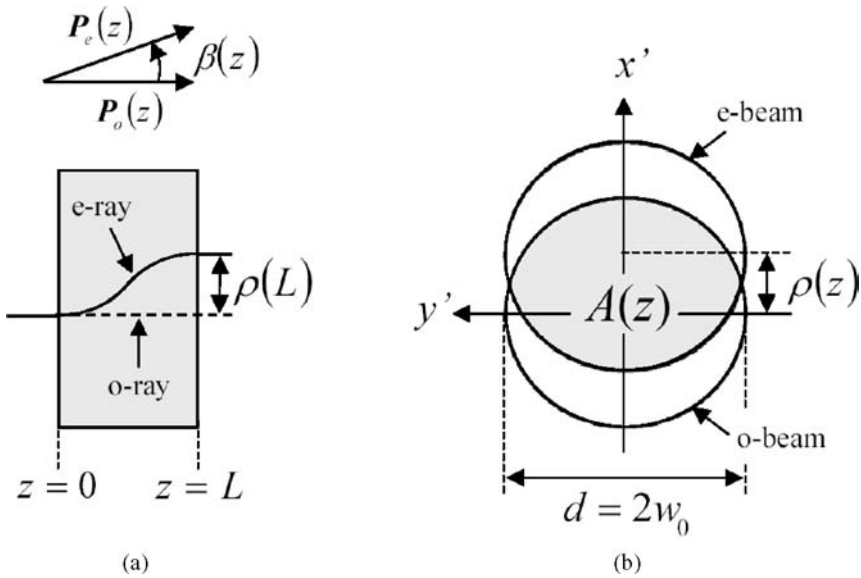

FIGURE 5 (a) Representation of the Poynting flux lines (light rays in geometrical optics) for the *o*-wave (dashed line) and the *e*-wave (solid line) when the liquid crystal film is reoriented. An angle $\beta(z)$ is made between the *o*- and *e*-Poynting vectors $\mathbf{P}_o(z)$ and $\mathbf{P}_e(z)$. The walk-off at location z in the film is denoted as $\rho(z)$. (b) Cross section of the *o*- and *e*-beams of diameter d at location z in the basis (x', y') which is obtained from the rotation of (x, y) by an angle Φ. The shaded area $A(z)$ is the overlap area.

situation that gives [21] $\tan\beta(z) = \varepsilon_a \sin 2\Theta / \left[2\left(\varepsilon_\perp + \varepsilon_a \cos^2\Theta\right)\right]$ where $\varepsilon_{ij} = \varepsilon_\perp \delta_{ij} + \varepsilon_a n_i n_j$ is the dielectric tensor at optical frequency and $\varepsilon_a = \varepsilon_{||} - \varepsilon_\perp$ is the corresponding anisotropy. In fact, the overlap mismatch between the *o*- and *e*-waves depends not only on the geometrical ratio δ but also on the reorientation amplitude Θ. It is then possible to define a typical value δ_c below which sizeable walk-off appears for a given Δ, say a mismatch of the overlap areas of the order of 10%, i.e. $[A(0) - A(L)]/A(0) \cong 0.1$. Similarly, we define the typical phase shift Δ_c above which walk-off effects are important for a given δ. For example, in the case of a circularly polarized excitation, it is known that $\Delta \cong \pi$ not too far above the Fréedericksz transition, this gives $\delta_c \cong 0.35$ for $L = 100\,\mu\text{m}$. From this point of view, it would appear that this value allows us to understand the experimental observations we have made around $\delta \cong 0.25$.

Finally, these results give a interesting starting point in the search for a quantitative interpretation of many complex dynamics observed in various interaction geometries, which are still unexplained when finite

beam size is neglected. Two examples will suffice to illustrate this point. We can first evaluate the critical values Δ_c that correspond to other experimental works in the field of light-induced reorientation dynamics. For instance, in the case of an ordinary excitation beam at oblique incidence the limitations of the IPW theoretical model [15], when compared to experimental data [12,14,26–28], may be understood since in these studies $\Delta_c/2\pi \cong 2-3$ but many rings are involved, implying $\Delta \gg \Delta_c$. Another example is the case of an astigmatic excitation beam (i.e. elliptical intensity profile) at normal incidence where intriguing complex dynamics were observed [16,17]. There, the corresponding critical phase shift verifies $\Delta_c/2\pi < 1$ although the reorientation is rather large ($\Delta \gg 1$).

CONCLUSION

We have analyzed the influence of the finite beam size on optically induced dynamics in nematic liquid crystals in the framework of circularly polarized light normally incident on an homeotropic NLC sample. In particular, the occurrence of intermittency, self-organization and possibly chaos has been reported. A mechanism based on walk-off between the ordinary and extraordinary waves has also been proposed and its implication has been discussed in the framework of various interaction geometries. A quantitative model has been recently derived in the case of circularly polarized excitation [29]. This approach may be fruitful for further quantitative discussions in many other interaction geometries known to exhibit complex dynamics.

REFERENCES

[1] Tabiryan, N. V., Sukhov, A. V., & Zel'dovich, B. Y. (1986). *Mol. Cryst. Liq. Cryst.*, *136*, 1.
[2] Khoo, I. C. & Wu, S. T. (1993). *Optics and nonlinear optics of liquid crystals*, World Scientific: Singapore.
[3] Santamato, E. (1995). *Nonlinear optical material and devices for applications in Information technology*, Kluwer Academic: Dordrecht.
[4] Simoni, F. (1997). *Nonlinear optical properties of liquid crystals and PDLC*, World Scientific: Singapore.
[5] Zolot'ko, A. S., Kitaeva, V. F., Kroo, N., Sobolev, N. N., & Csillag, L. (1980). *Pis'ma Zh. Eksp. Teor. Fiz.*, *32*, 170. [JETP Lett. 32, 158 (1980)].
[6] Zolot'ko, A. S., Kitaeva, V. F., Kuyumchyan, V., Sobolev, N., Sukhorukov, A., & Csillag, L. (1982). *Pis'ma Zh. Eksp. Teor. Fiz.*, *36*, 66. [JETP Lett. 36, 80 (1982)].
[7] Zel'dovich, B. Y. & Tabiryan, N. (1979). *Pis'ma Zh. Eksp. Teor. Fiz.*, *30*, 510. [JETP Lett. 30, 478 (1980)].
[8] Marrucci, L., Abbate, G., Ferraiuolo, S., Maddalena, P., & Santamato, E. (1992). *Phys. Rev. A*, *46*, 4859.

[9] Vella, A., Piccirillo, B., & Santamato, E. (2002). *Phys. Rev. E*, *65*, 031706.
[10] Brasselet, E., Doyon, B., Galstian, T. V., & Dubé, L. J. (2002). *Phys. Lett. A*, *299*, 212.
[11] Brasselet, E., Doyon, B., Galstian, T. V., & Dubé, L. J. (2003). *Phys. Rev. E*, *67*, 031706.
[12] Cipparrone, G., Carbone, V., Versace, C., Umeton, C., Bartolino, R., & Simoni, F. (1993). *Phys. Rev. E*, *47*, 3741.
[13] Tabiryan, N. V., Tabiryan-Murazyan, A. L., Carbone, V., Cipparrone, G., Umeton, C., Versace, C., & Tschudi, T. (1998). *Opt. Comm.*, *154*, 70.
[14] Santamato, E., Maddalena, P., Marrucci, L., & Piccirillo, B. (1998). *Liq. Cryst.*, *25*, 357.
[15] Demeter, G. & Kramer, L. (1999). *Phys. Rev. Lett.*, *83*, 4744; Demeter, G. (2000). *Phys. Rev. E*, *61*, 6678; Demeter, G. & Kramer, L. (2001). *Phys. Rev. E*, *64*, 020701.
[16] Piccirillo, B., Toscano, C., Vetrano, F., & Santamato, E. (2001). *Phys. Rev. Lett.*, *86*, 2285.
[17] Vella, A., Setaro, A., Piccirillo, B., & Santamato, E. (2003). *Phys. Rev. E*, *67*, 051704.
[18] Zel'dovich, B. Y. & Tabiryan, N. (1982). *Zh. Eksp. Teor. Fiz.*, *82*, 1126 [Sov. Phys. JETP 55, 656 (1982)].
[19] Khoo, I. C., Liu, T. H., & Yan, P. Y. (1987). *J. Opt. Soc. Am. B*, *4*, 115.
[20] Romanov, V. P. & Fedorov, D. O. (1995). *Opt. Spektrosk.*, *78*, 274 [Opt. Spectrosc. (USSR) 78, 244 (1995)]; Romanov, V. P. & Fedorov, D. O. (1995). *Opt. Spektrosk.*, *79*, 313 [Opt. Spectrosc. (USSR) 79, 288 (1995)].
[21] Brasselet, E., Doyon, B., Galstian, T. V., & Dubé, L. J. (2004). *Phys. Rev. E*, *69*, 0117xx.
[22] Brasselet, E. & Galstian, T. V. (2000). *Opt. Comm.*, *186*, 291.
[23] Zolot'ko, A. S. & Sukhorukhov, A. P. (1990). *Pis'ma Zh. Eksp. Teor. Fiz.*, *52*, 707 [JETP Lett. 52, 62 (1990)].
[24] Brasselet, E. & Galstian, T. V. (2001). *Opt. Comm.*, *200*, 241.
[25] Santagiustina, M., Colet, P., SanMiguel, M., & Walgraef, D. (1998). *Phys. Rev. E*, *58*, 3843.
[26] Russo, G., Carbone, V., & Cipparrone, G. (2000). *Phys. Rev. E*, *62*, 5036.
[27] Cipparrone, G., Russo, G., Versace, C., Strangi, G., & Carbone, V. (2000). *Opt. Comm.*, *173*, 1.
[28] Carbone, V., Cipparrone, G., & Russo, G. (2001). *Phys. Rev. E*, *63*, 051701.
[29] Brasselet, E. (2004). *Phys. Lett. A*, accepted.